Uniform 90-channel multiwavelength InAs/InGaAsP quantum dot laser

Liu, J.; Lu, Z.; Raymond, S.; Poole, Philip; Barrios, P. J.; Pakulski, Grzegorz; Poitras, Daniel; Xiao, George; Zhang, Z.

Publisher's version / Version de l'éditeur:
https://doi.org/10.1049/el:20070594
Electronics Letters, 43, 8, pp. 458-460, 2007-04-12

Uniform 90-channel multiwavelength InAs/InGaAsP quantum dot laser

Jiaren Liu, Zhenguo Lu, S. Raymond, P.J. Poole, P.J. Barrios,
G. Pakulski, D. Poitras, George Xiao, and Zhiyi Zhang
Institute for Microstructural Sciences, National Research Council,
Ottawa, ON, Canada K1A 0R6

Abstract

A 93-channel multi-wavelength laser with maximum channel intensity non-uniformity of 3.0-dB over a wavelength range from 1638nm to 1646nm was demonstrated on the basis of a single 4500 μm-long InAs/InGaAsP quantum dot Fabry-Perot (F-P) cavity chip. All channels were stable because of inhomogeneous gain broadening due to statistically distributed sizes and geometries of self-assembled quantum dots.

Key words: quantum dot, semiconductor laser, multi-wavelength laser

Introduction:

Multi-wavelength laser sources have potential applications in wavelength-division multiplexing (WMD), sensing, metrology, testing, and spectroscopy. Several gain mechanisms such as rare-earth-doped fiber amplification [1-2], bulk or quantum-well semiconductor optical amplification [3-4] and stimulated Raman scattering [5], have successfully been employed to simultaneously generate multi-wavelength outputs. However, the resulting multi-wavelength lasers without additional gain equalization have not performed well in term of channel number, intensity uniformity and stability mostly due to the use of homogeneous gain materials. In order to overcome this problem, we explore possibilities to develop a multi-wavelength semiconductor laser with quantum dots (QDs) in this paper. QD-based semiconductor is promising material for next-generation high-speed optical communication devices. Lasers based on semiconductor QDs have already demonstrated better optical performance such as low threshold current densities [6], small chirp [7], wide tunability [8], and passive mode-locking [9]. The suitability of QD lasers for multi-wavelength operation with better performance lies in the facts such as spectral hole-burning in very broad inhomogeneous gain of QDs and spatial hole-burning in a semiconductor F-P cavity. In a InAs/InGaAsP QD material system, inhomogeneous broadening of gain spectrum stems from statistically distributed sizes and geometries of self-assembled QDs, and its 3-dB bandwidth of up to 150 nm could be easily achievable [12, 8], which provides a base for uniform and stable multi-channel operation. Each of lasing modes selected by a semiconductor F-P cavity extracts only electrons in QDs resonant with the wavelength of that mode, depletes electrons in these QDs with the corresponding dot sizes, and accordingly, mode gain is saturated. Because QDs are spatially isolated and only interact via wetting layers, the supply of electrons that remain in the material surrounding QDs helps the realization of ultrafast gain recovery to suppress gain fluctuation. Consequently, each mode consumes population inversion of differently localized carriers. This fast-recovery ultra-wide inhomogeneous broadening, as well as traditional spatial hole-burning inside a standing-wave cavity, will principally support multi-wavelength operation with high channel number and high uniformity of channel intensities.

Experiment results and discussions:

InAs/InGaAsP *p-i-n* quantum dot laser diodes used in the experiments were grown by chemical beam epitaxy (CBE) on exactly oriented (100) InP *n*-type substrates. The undoped active region of the lasers consisted of five stacked layers of self-assembled InAs QDs embedded in quaternary $In_{0.816}Ga_{0.184}As_{0.392}P_{0.609}$ (1.15Q) layers resulting in a total thickness of about 400nm. From transmission electron microscopy (TEM) measurements, the QD density in each QD layer was approximately $5\times10^{10}\,cm^{-2}$. Optical confinement in the lateral direction was achieved by a planar waveguide configuration while this aforementioned core in the vertical direction was surrounded with a *n*-InP bottom cladding layer and a *p*-InP top cladding layer. The latter cladding was covered with a cap of $p^{+}-In_{0.522}Ga_{0.478}As$ to ensure good ohmic contact to the top metal stack. More details about the growth of these structures and other optical characteristics can be found in our published papers [8, 10].

The QD ridge waveguide laser sample was cleaved perpendicularly to the diode junction plane, at a length of $4500 \pm 2\mu m$. Both of the laser end facets were left uncoated and their reflectivity estimated to be approximately 30%. The laser chip itself is served as an active medium, a filter for longitudinal modes, a polarization maintaining component, and cavity mirrors as well. The laser output at one facet was coupled by a special fiber with numerical aperture of 0.35 and mode field diameter of $4.0\mu m$, and sent to an optical spectrum analyzer (OSA) (Ando AQ6317B) and/or a power meter through a SMF-28 fiber spliced with that special fiber. The QD laser sample was mounted on a TEC cooler at a temperature of $17.00 \pm 0.01^{\circ} C$, and driven by CW injection current.

For lasing threshold measurement, the output power of this QD laser after the SMF-28 fiber was monitored as a function of the biased current as shown in Fig.1. The onset of lasing corresponds to the threshold current of about 152mA. Below the lasing threshold, the amplified spontaneous emission (ASE) at 110mA as shown in Fig.2 has a 3-dB bandwidth of 65.6nm and 1-dB bandwidth of 34.8nm, respectively. This flat ASE spectrum is critical for multiple-wavelength lasing operation, which supports many lasing line oscillations simultaneously. Far above the lasing threshold, Fig.3 shows a typical spectrum of quantum dot laser as a function of wavelength in the case of $2.0\mu m$ wide ridge and $4500\mu m$ long cavity with the injection current $260mA$. The OSA resolution was set at 10pm. 93 lasing peaks were simultaneously observed over the 8-nm wavelength window from 1638nm to 1646nm. The maximum intensity non-uniformity of the lasing modes was about 3.0dB while their minimum signal-to-noise ratio (SNR) was 25.0dB. The channel spacing at the center wavelength 1642nm was estimated to be 86.0 pm (or 9.56 GHz). Theoretically, the channel spacing, $\Delta\lambda(\lambda) = \lambda^2 / [2.n_{eff}(\lambda, T, J).L]$, is determined by the cavity length L and the effective refractive index $n_{eff}(\lambda, T, J)$ where λ, T, and J are denoted as vacuum wavelength, temperature, and effective current density respectively; therefore, it is varying as a function of intracavity waveguide dispersion. Experimentally, it was changed from 85.2 pm (or 9.52 GHz) at 1638nm to 86.8 pm (or 9.61 GHz) at 1646nm. This small but nontrivial spacing irregularity could be ameliorated mostly or corrected completely by designing the dispersion of ridge waveguides. From these data, the effective refractive index $n_{eff}(\lambda, T, J)$ and the facet reflectivity R at $17^{\circ}C$ and $260mA$ were calculated to be 3.4834 and 30.7% at 1642nm respectively. While the output power of each channel at the OSA with the 10-pm resolution was larger than $5.0\mu w$, it was measured to be $\geq 30.0\mu w$ per facet just at the front of the facets. The difference is largely due to laser-fiber coupling loss, fiber-splicing loss, and loss related to high-resolution OSA measurement.

Conclusions

The single $4500\mu m$-long InAs/InGaAsP quantum dot Fabry-Perot (F-P) cavity monolithic chip was fabricated and tested. It was used to generate a 93-channel multi-wavelength laser with 86-pm channel spacing, minimum SNR of 25dB, and maximum channel intensity non-uniformity of 3-dB over the wavelength range from 1638nm to 1646nm. This is the first time, to the best of our knowledge, to demonstrate the multi-wavelength lasing operation with such a simple monolithic QD chip without any external components such as filters, polarization controllers and reflectors. Its channel spacing could be easily controlled by precisely cutting of waveguide lengths, its threshold current density dramatically reduced by high-reflectivity coatings at one or two end facets, and its SNR further improved by eliminating high-order spatial mode(s) that broaden laser mode linewidths and fill in spectral minima. Conclusively, monolithic multi-wavelength QD lasers have potentials to become import but simple and cost-effective optical sources.

References

[1] A. Bellemare, M. Karasek, M. Rochette, S. LaRochelle, and M. Tetu, "Room temperature multifrequency erbium-doped fiber lasers anchored on the ITU frequency grid," J. Lightwave Technol. **18**, 825-831 (2000).

[2] S. Yamashita, and K. Hotate, "Multiwavelength erbium-doped fiber laser using intracavity etalon and cooled by liquid nitrogen," Electron. Lett. **32**, 1298-1299 (1996).

[3] H. Chen, "Multiwavelength fiber ring lasing by use of a semiconductor optical amplifier," Opt. Lett.**30**, 619-621 (2005).

[4] M. T. Hill, T.de Vries, H. J. S. Dorren, X. J. M. Leijtens, J. H. C. van Zantvoort, J. H. den Besten, E. Smalbrugge, Y. S. Oei, J. J. M. Binsma, G. D. Khoe, and M. K. Smit, "Integrated two-state AWG-based multiwavelength laser," IEEE Photonics Technol. Lett. **17**, 956-958 (2005).

[5] X. Dong, P. Shum, and N. Q. Ngo, "Multiwavelength Raman laser with a continuously- tunable spacing," Optics Express **8**, 3288-3293 (2006).

[6] G. Park, O. B. Shchekin, D. L. Huffaker, and D. G. Deppe, "Low-threshold oxide-confined 1.3- μm quantum dot laser," IEEE Photonics Technol. Lett. **13**, 230-232 (2000).

[7] H. Saito, K. Nishi, A. Kamei, and S. Sugou, "Low chirp observed in directly modulated quantum dot lasers," IEEE Photonics Technol. Lett. **12**, 1298-1300 (2000).

[8] G. Ortner, C. N. Allen, C. Dion, P. Barrios, D. Poitras, D. Dalacu, G. Pakulski, J. Lapointe, P. J. Poole, W. Render, and S. Raymond, "External cavity InAs/InP quantum dot laser with a tuning range of 166nm," Applied Phys. Lett. **88**, 121119 (2006).

[9] X. Huang, A. Stintz, H. Li, L. F. Lester, J. Cheng, and K. J. Malloy, "Passive mode-locking in 1.3- μm two-section InAs quantum lasers," Applied Phys. Lett. **19**, 2825-2827 (2001).

[10] Z. G. Lu, J. R. Liu, S. Raymond, P. J. Poole, P. J. Barrios, D. Poitras, F. G. Sun, G. Pakulski, P. J. Bock, and T. Hall, "Highly efficient non-degenerate four-wave mixing process in InAs/InGaAsP quantum dots," Electron. Lett. **42**, 1112-1113 (2006).

[11] B. W. Hakki and T. L. Paoli, "Gain spectra in GaAs double-heterostructure injection lasers," J. Appl. Phys. **46**, 1299-1306 (1975).

[12] Z. G. Lu, J. R. Liu, S. Raymond, P. J. Poole, P. J. Barrios, G. Pakulski, D. Poitras, F. G. Sun, S. Taebi, and T. Hall, "Ultra-broadband quantum-dot semiconductor amplifier and its applications," OFC 2007, JThA33 92007).

Captions

FIG.1. L-I curve of the QD laser with the lasing threshold current of about 152mA.

FIG.2. ASE at 110mA with a 1-dB bandwidth of 34.8nm and a 3-dB bandwidth of 65.6nm

FIG.3. Spectrum of the multiwavelength QD laser with 86.0-pm channel spacing and maximum channel intensity non-uniformity of 3.0-dB over the wavelength range 1638nm - 1646nm at $17^{\circ}C$ and $260mA$. The laser had a length of $4500\mu m$ and a width of $2.0\mu m$.

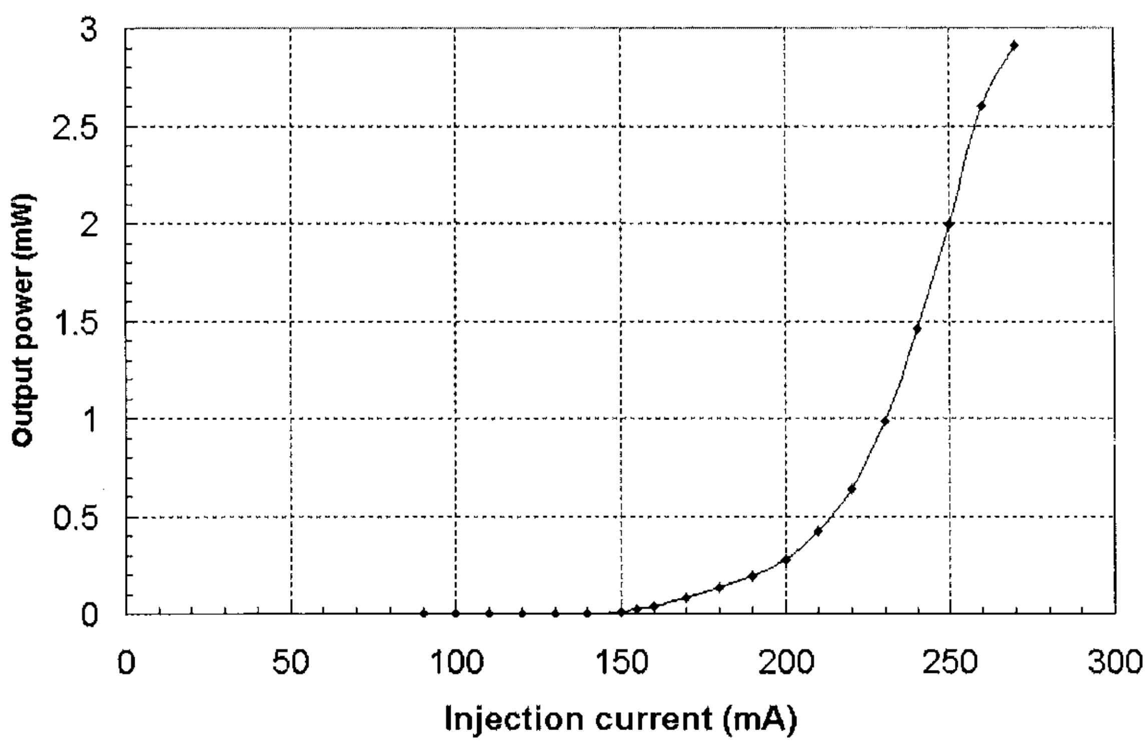

FIG.1

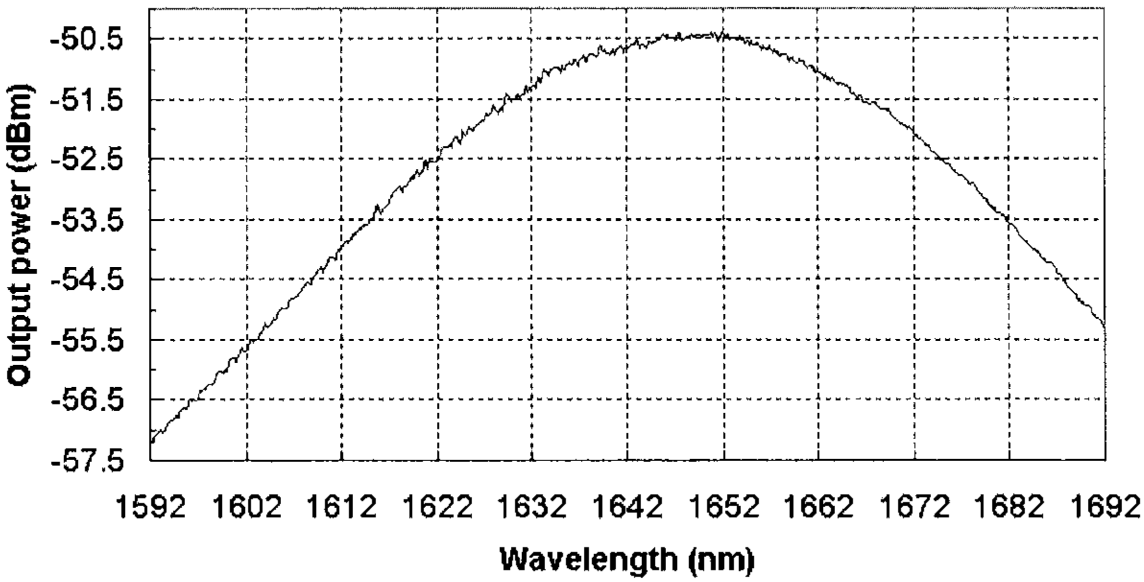

-50.5
-51.5
-52.5
-53.5
-54.5
-55.5
-56.5
-57.5
Output power (dBm)
1592
1602
1612
1622
1632
1642
1652
1662
1672
1682
1692
Wavelength (nm)

FIG.2.

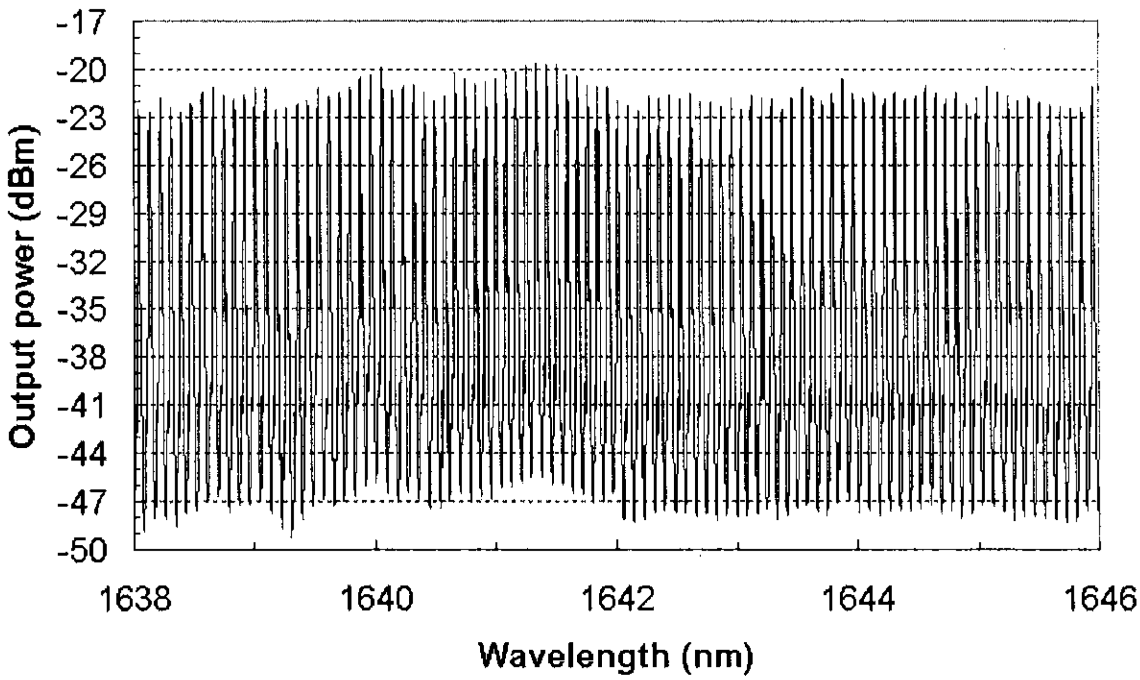

-17
-20
-23
-26
-29
-32
-35
-38
-41
-44
-47
-50
Output power (dBm)
1638
1640
1642
1644
1646
Wavelength (nm)

FIG. 3